

# Rhodamine B Adsorption on Natural and Modified Moroccan Clay with Cetyltrimethylammonium Bromide: Kinetics, Equilibrium and Thermodynamics

B. Damiyine\*, A. Guenbour, R. Boussen\*

Laboratory of Materials Nanotechnology and Environment, Department of Chemistry, Faculty of Science, University Mohammed V, BP1014, Rabat, Morocco.

Received 20 Oct 2016

Revised 5 Feb 2017

Accepted 5 Feb 2017

Keywords :

- Natural Clay,
- Rhodamine B,
- Langmuir,
- Adsorption isotherm,
- Kinetics studies,
- Sorption

[ratiba20@gmail.com](mailto:ratiba20@gmail.com);

Phone: +2126

60614610Brahimgp@gm

ail.com; Phone: +212 6

61950835

## Abstract

The use of raw and modified Moroccan natural clays as adsorbent for sewage treatment was investigated for the removal availability of textile dyes from aqueous solution. For this purpose, the adsorption of Rhodamine B (RB) by raw (RC) and modified clay (MC), were investigated through batch adsorption experiment. The clays were characterized by means of XRD, Energy-dispersive X-Ray spectroscopy (EDX) and Fourier transformed infrared spectroscopy (FTIR). The effects of initial dye concentration, contact time, solution temperature and pH solution on kinetic parameters are discussed. The adsorption process was followed by UV-spectrophotometric technique in a specially designed adsorption cell. Thermodynamic studies and adsorption isotherms Langmuir, Freundlich and Temkin models were used to describe this phenomenon of adsorption and to obtain isotherm parameters. The results showed that sorption process was best described by the pseudo-second-order model and which were more favorable at higher pH. Increase in temperature from 25 to 55°C of RB adsorption on both RC and MC increased, the degree of dispersion and the process was found to be physisorptive and endothermic for MC and RC, this was obtained from the thermodynamic studies. The quantity eliminated was depended on the initial concentration, contact time, solution temperature and pH of solution. The results showed that MC can be used adequately to adsorb RB more efficiently than RC.

## 1. Introduction

Rapid industrialization causes significant increase of wastewater, especially, organic pollution and dye industry effluent cause risk to human health and ecological balance.

For this purpose, many methods such as activated carbon sorption, chemical coagulation, ion exchange, electrolysis, biological treatment and others, have been developed [1] [2] to eliminate undesirable pollution.

The present study is aimed to study a convenient and economic method for RB removal from water by adsorption on a low cost and an abundantly available adsorbent, to gain an understanding of the adsorption kinetics, to describe the rate and mechanism of adsorption, to determine the factors controlling the rate of adsorption and to calculate the activation energy of system. The effects of solution pH, initial concentration, contact time and solution temperature on RB adsorption rate have been evaluated.

## 2. Materials and methods

### 2.1. Preparation of the CTAB/CLAY adsorbents

Ten g of raw clay (RC) was extracted from a quarry that is located in the "Shoul" region (Morocco). The RC sample was sieved by 90-mesh sieve and dried at 110°C for 1 h.

The RC sample was stirred vigorously in 20 ml of absolute ethanol for 12 h, the washed clay was then harvested by vacuum filtration and dried in a static air oven at 90°C for 4 h. The dried clay (10g) was suspended in 150 ml of 0.1 M CTAB (aqueous) and stirred with a magnetic stirrer at 500 rpm for 2 h [3].

The resultant CTAB/CLAY was harvested from the suspension by vacuum filtration and washed several times with distilled water to eliminate excess CTAB prior to drying in an oven at 115°C for 4 h.

The cetyltrimethylammonium bromide (C<sub>19</sub>H<sub>42</sub>BrN) purchased from AppliChem GmbH, Germany.

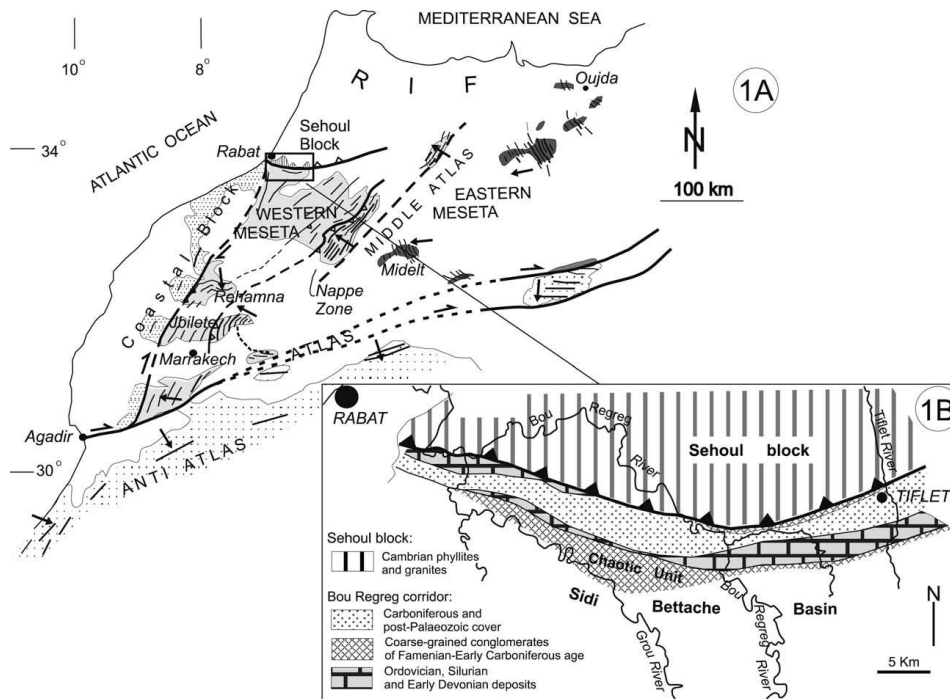


Figure 1: Geological map of the investigated area [4]

## 2.2. Characterization of the adsorbents

The chemical composition of the RC and MC, which was determined by XRD on a Siemens d5000 X-Ray diffractometer (figure 2) shows that quartz “SiO<sub>2</sub>” and calcite “CaCO<sub>3</sub>” are the major molecules of clay studied.

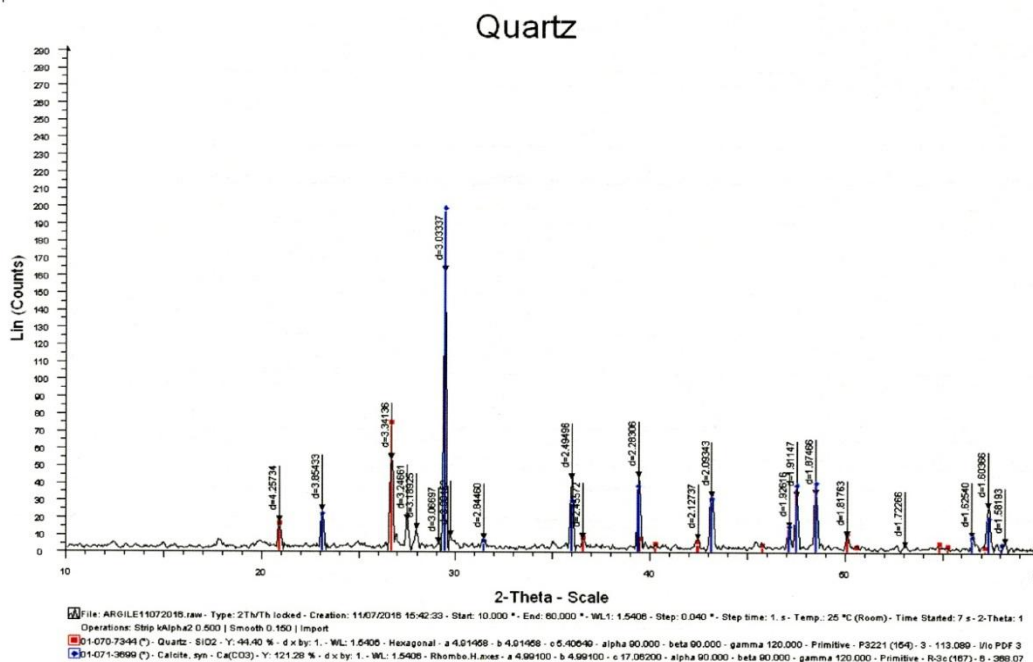
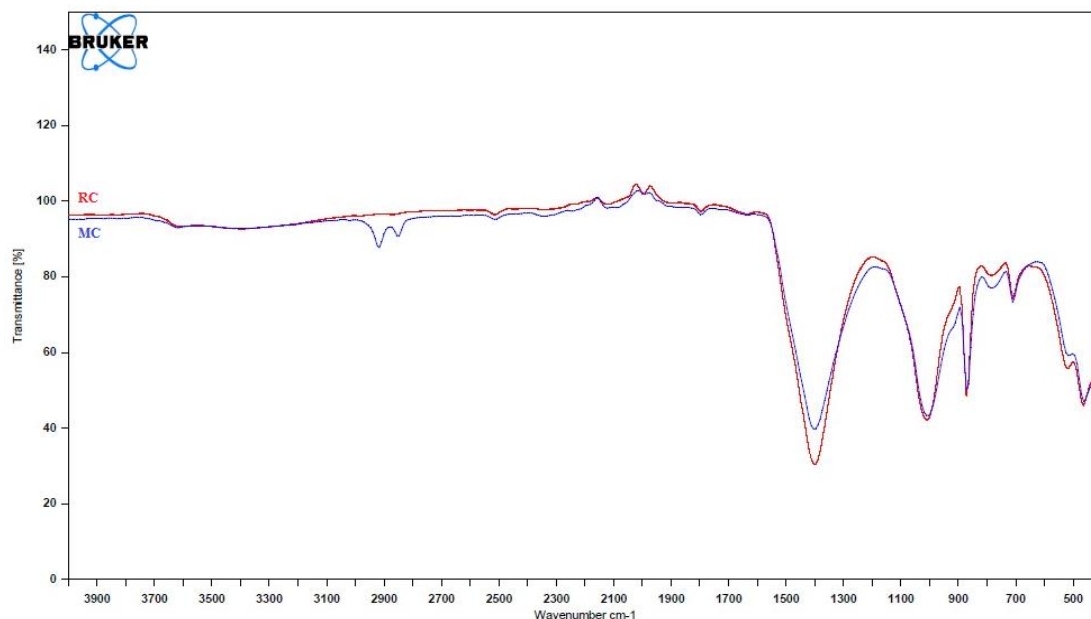


Figure 2: XRD spectrum of raw clay.

The FT-IR spectra were recorded at 400–4000 cm<sup>-1</sup> wavenumber range using a FT-IR spectrometer (BRUKER, model: Tensor 27) (figure 2), The bands of wavelength 1399.95 cm<sup>-1</sup>, 870.03 cm<sup>-1</sup> and 708.85 cm<sup>-1</sup> are bands characteristics of the calcium carbonate, and the band of wavelength 1009,13 cm<sup>-1</sup> is a band characteristic of the silicon [5].

The bands of wavelength 2921 cm<sup>-1</sup> and 2853 cm<sup>-1</sup> are the bands characteristics of cetyltrimethylammonium bromide [6].



**Figure 3:**FTIR spectrum of raw and modified clay

The Energy Dispersive X-Ray (EDX) analysis was performed using HORIBA XGT-1000 (Figure 4 and Table 1). The RC and MC after and before adsorption images were carried out by digital microscope Leica DVM5000 HD (figure 5).

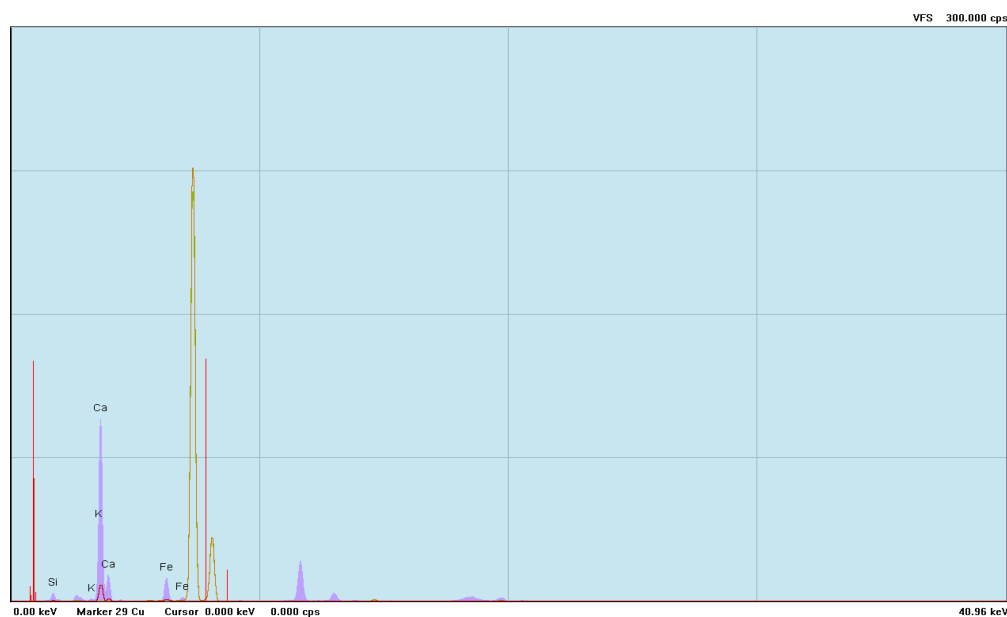


**Figure 4:** EDX spectrum of raw clay

**Table 1:** Chemical composition of raw clay

Major Elements	Composition (Wt %)
Ca	77.97
Si	11.46
Fe	7.74
Al	1.98
K	0.85

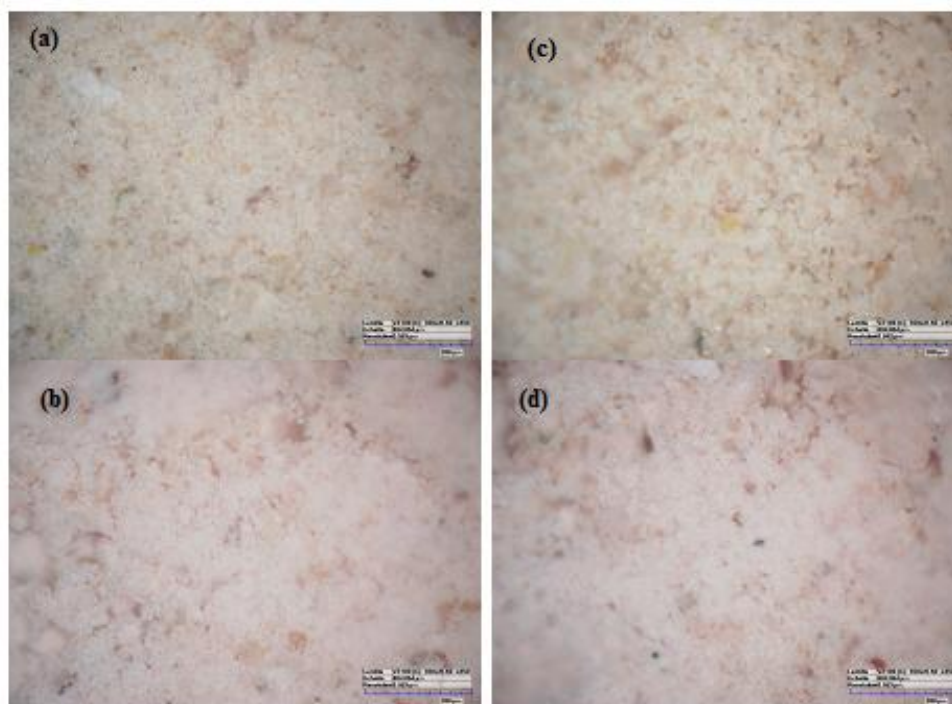


**Figure 5:** Digital Microscopy images of RC before (a) after adsorption (b) and of MC before (c) after (d) adsorption

### 2.3. Rhodamine B

Rhodamine B is a cationic dye, purchased from Merck Millipore Corporation, Germany. The structure of dye is shown in Figure 6. The absorbance maximum is 554 nm.

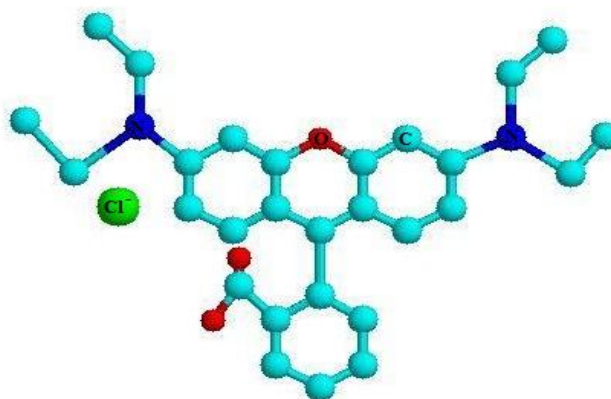


**Figure 6:** Structural formula of Rhodamine B

The batch adsorption experiments were carried by adding 0.01 g of adsorbent into 250 mL Erlenmeyer flasks containing 50 mL of different initial concentrations of RB solution. The flasks were agitated with a magnetic stirrer at 500 rpm. The adsorbent was separated and centrifuged at 3000 rpm for 15 min, the concentration of RB in supernatant was determined at a wavelength of maximum adsorption ( $\lambda_{max}$ ) at 554 nm by visible spectrophotometer (Jasco V-670 spectrophotometer). The amount of adsorbed dye at equilibrium  $q_e$  (mg/g) and the removal percentage were calculated by the following equations:

$$q_e = (C_0 - C_e) \cdot V / W \quad (1)$$

$$\% \text{ removal} = ((C_0 - C_e) / C_0) \times 100 \quad (2)$$

Where  $C_0$  and  $C_e$  are the initial and equilibrium concentrations of dye, respectively (mg/L).  $V$  is the volume of dye solution (L) and  $W$  is the weight of adsorbent used (g).

### 3. Results and discussion

#### 3.1. Effect of contact time

Figure 7 and 8 shows the adsorption percentage of RB as a function of contact time. As seen in this figures, adsorption of this dye increased by contact time and reached to a maximum value 83.95 % for RC with concentration 20 mg/l and 90.10 % for MC with same concentration. More increase in contact time had more sensible changes in adsorption percentage. Hence, adsorption of RB reached their maximum at 30 and 270 min, respectively. These values have been selected as optimum contact time.

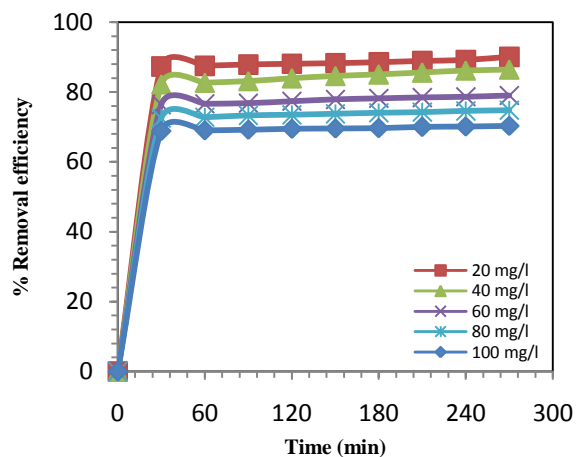
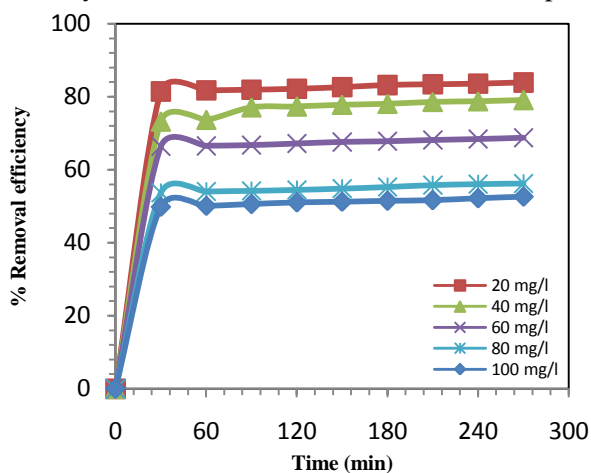


**Figure 7:** Effect of contact time on adsorption of RB onto RC.

**Figure 8:** Effect of contact time on adsorption of RB onto MC.

(Adsorbent dose = 0.01 g/50 mL, T=25°C)

#### 3.2. Effect of pH

The pH of the dye solution is one of the most important parameter as the protonation of functional groups on adsorbent surface and the chemistry of dye molecules are strongly affected by pH of the solution. The effect of initial pH on the adsorption of RB by RC and MC was studied by varying the pH of dye solution from 2 to 12 for initial concentration of 20 mg/L (Figure 9 and 10).

It is evident from the figure that the sorption capacity of RC increased from 81.70 % to 82.10 % with increase in solution pH 2 to 12, and for MC the sorption capacity increased from 87.50 % to 88.20 % with increase in solution pH 2 to 12.

Therefore, the pH for 7 to 12 was selected as an optimum pH for this experiment.

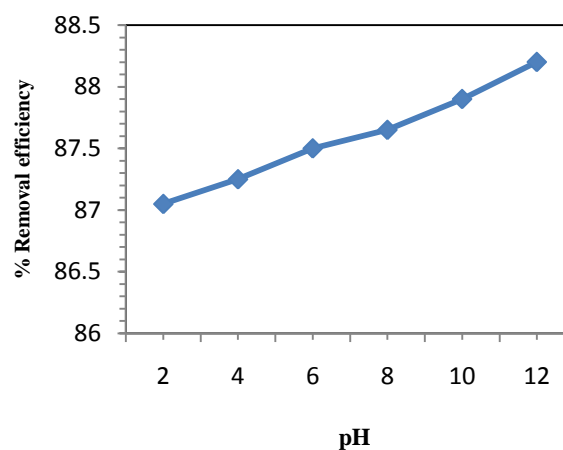
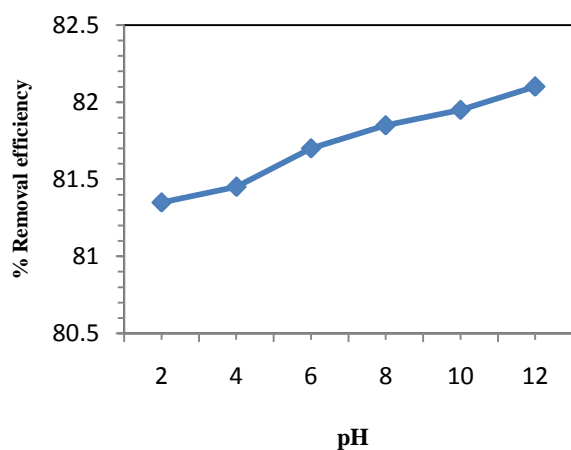


**Figure 9:** The effect of pH on the removal of RB onto RC.

**Figure 10:** The effect of pH on the removal of RB onto MC.

(Adsorbent dose = 0.01 g/50 mL, C = 20 mg/L, t = 60 min, T=25°C).

#### 3.3. Effect of temperature

The results of the studies on the influence of temperature on RB adsorption are presented in figures 11 and 12. The batch mode adsorption studies were carried out to study the effect of temperature for the removal of RB dye. Batch adsorption experiments were carried by adding 0.01 g of clay into 250 mL in Erlenmeyer flasks containing 50 mL of solution at different temperature 25°C, 35°C, 45°C and 55 °C.

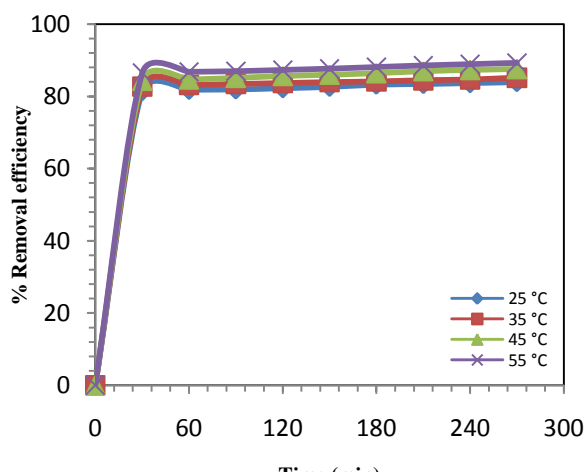


**Figure 11:** Effect of temperature on the adsorption kinetics of RB onto RC (Adsorbent dose = 0.01 g/50 mL)

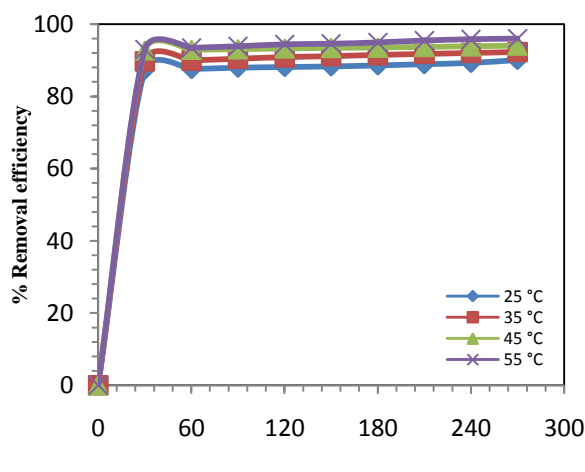


**Figure 12:** Effect of temperature on the adsorption kinetics of RB onto MC (Adsorbent dose = 0.01 g/50 mL)

A study of the temperature dependence of adsorption reactions gives valuable information about the enthalpy and the entropy change during adsorption. The adsorption of both clay indicating that the phenomenon of removal of RB is endothermic in nature when temperature was increased from 25 to 55°C at pH neutral and  $C_0 = 20\text{mg/L}$ . The increase in the equilibrium sorption of dye with temperature indicates that dye removal by adsorption on RC and MC favor's at high temperature [7]. This may be a result of increase in the mobility of the large dye ion with temperature.

An increasing number of molecules may also acquire sufficient energy to undergo an interaction with active sites at the surface. Furthermore, increasing temperature may produce a swelling effect within the internal structure of the clay enabling large dyes to penetrate further [8].

#### 3.4. Effect of the initial concentration of dye

The effect of initial concentration on RB removal by studied adsorbents is shown in (Figure 13 and 14). It can be seen that the adsorption capacity of RB dye by studied adsorbents increase with increase in the initial RB dye concentration, and then approaches a fixed value. The increase of adsorption capacity with raising the initial RB dye concentration is due to an increase of the numbers of RB dye molecule available to binding sites of adsorbents. At higher RB dye concentration, the active sites become saturated and adsorption capacity approaches a constant value.

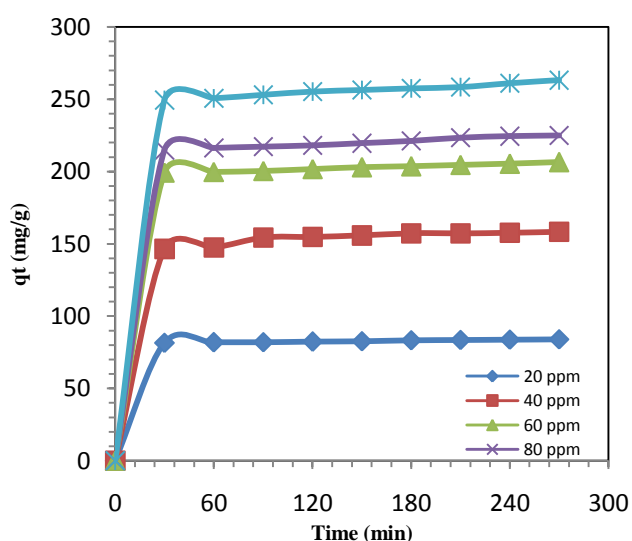


**Figure 13:** Effect of concentration of RB on adsorption onto RC (Adsorbent dose = 0.01 g/50 mL,  $T=25^\circ\text{C}$ ).

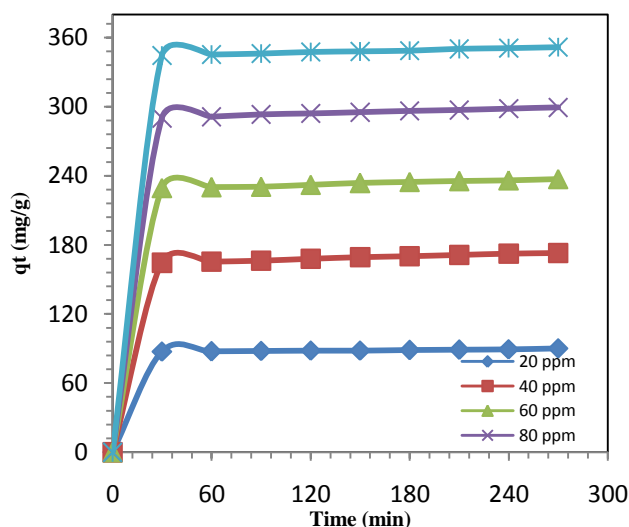


**Figure 14:** Effect of concentration of RB on adsorption onto MC (Adsorbent dose = 0.01 g/50 mL,  $T=25^\circ\text{C}$ ).

### 3.5. Adsorption isotherm

The adsorption isotherm represents the quantity adsorbed according to the concentration of the aqueous solution to equilibrium at a given temperature. Firstly the isotherms models of adsorption are generally used to describe the interactions between the adsorbate and the adsorbent when the process of adsorption reaches equilibrium. Secondly, they make it possible to extract the important parameters for the systems design from adsorption. The data of adsorption were analyzed by three models of isotherms, Freundlich, Langmuir and Temkin.

#### 3.5.1. Langmuir adsorption isotherm

The Langmuir isotherm assumes monolayer adsorption on a uniform surface with a finite number of adsorption sites. Once a site is filled, no further adsorption can take place at that site. As such the surface will eventually reach a saturation point where the maximum adsorption of the surface will be achieved [9]. The linear form of the Langmuir isotherm model is described [10] as:

$$\frac{C_e}{Q_e} = \frac{1}{K_L Q_m} + \frac{1}{Q_m} C_e \quad (3)$$

Where  $C_e$  is the equilibrium concentration in the solution (mg/l),  $Q_e$  is the equilibrium uptake on the adsorbent (mg/g),  $Q_m$  is the maximum adsorption capacity (mg/g), and  $K_L$  is the Langmuir constant that is related to the affinity of binding sites and is related to the energy of sorption (l/g). These constants can be determined from the linear plot  $C_e/Q_e$  versus  $C_e$ , which has a slope of  $1/Q_m$  and the intercept of  $1/K_L Q_m$  (Figure 15 and 16).

From the regression correlation coefficient ( $R^2$ ) values that are regarded as a measure of the goodness of fit of experimental data on the isotherm's model (Table 2), it illustrates that the Langmuir equation represent RB adsorption process on RC and MC at the different solution temperatures very well, the  $R^2$  values is 0.9999 for RC and MC, indicating a good mathematical fit. On the other side it may be predicted from (Table 2) that the RB adsorption on the RC and MC is an endothermic process. Where monolayer sorption capacity of RB ( $Q_m$ ) increased as solution temperature was increased.

The essential characteristic of the Langmuir isotherm can be evidenced by the dimensionless constant called equilibrium parameter,  $R_L$ .

$$R_L = \frac{1}{1 + K_L C_0} \quad (4)$$

Where  $K_L$  is the Langmuir constant  $C_0$  is the initial RB concentration,  $R_L$  values indicate the type of isotherm to be irreversible ( $R_L = 0$ ), favorable ( $0 < R_L < 1$ ), linear ( $R_L = 1$ ) or unfavorable ( $R_L > 1$ ) [11].

In this study, all  $R_L$  values obtained for RC and MC were between 0 and 1 as shown in (Table 2). These values support the previous observation where the Langmuir isotherm was favorable for RB adsorption for all studied temperatures.

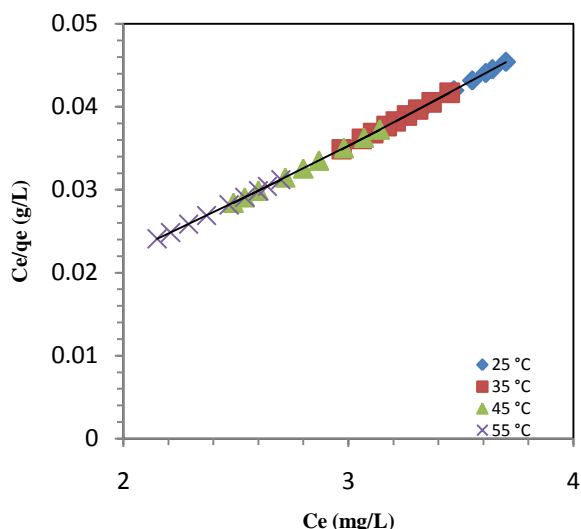


Figure 15: Langmuir isotherm for RB adsorption onto RC

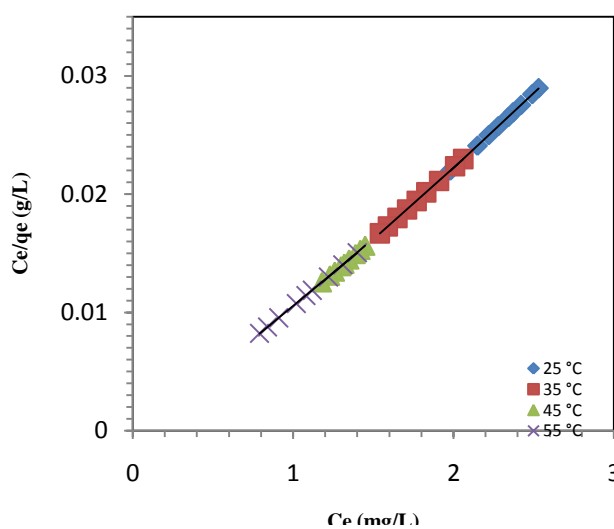


Figure 16: Langmuir isotherm for RB adsorption onto MC

### 3.5.2. Freundlich adsorption isotherm

The obtained experimental RB uptake values have also been analyzed using Freundlich equation. The Freundlich isotherm model is valid for multilayer adsorption on a heterogeneous adsorbent surface with a no uniform distribution of heat of adsorption. Freundlich isotherm can be expressed by: [12].

$$\log Q_e = \log K_F + \frac{1}{n} \log C_e \quad (5)$$

Where  $n$  and  $K_F$  are Freundlich constants related to adsorption intensity and adsorption capacity, respectively. The Freundlich constants  $K_F$  and  $n$  are obtained from the plot of  $\log Q_e$  versus  $\log C_e$  that should give a straight line with a slope of  $1/n$  and intercept of  $\log K_F$ . From (figure 17 and 18), a linear relation was observed among the plotted parameters at different temperatures.

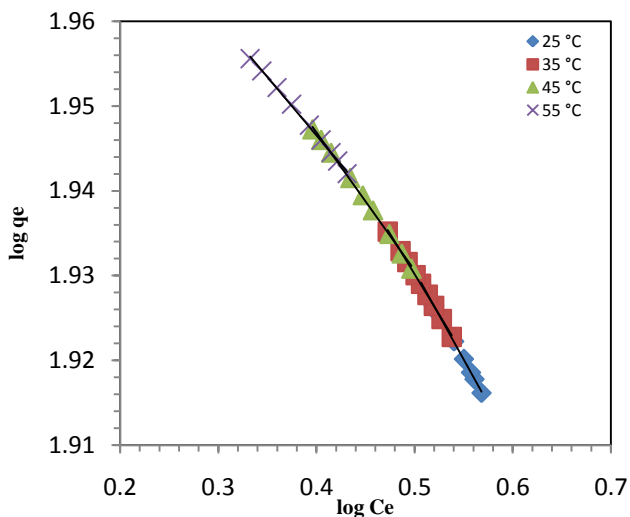


Figure 17: Freundlich isotherm for RB adsorption onto RC

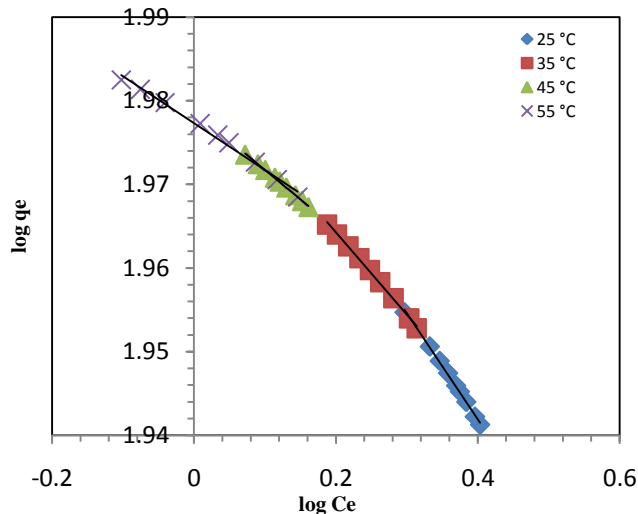


Figure 18: Freundlich isotherm for RB adsorption onto MC

### 3.5.3. Temkin adsorption isotherm

The Temkin isotherm model assumes the adsorption energy decreases linearly with the surface coverage due to adsorbent–adsorbate interactions. The linear form of Temkin isotherm model [13] is defined by:

$$Q_e = B \ln K_t + Bt \ln C_e \quad (6)$$

Where  $Bt$  is the Temkin constant related to heat of adsorption (KJ/mol) and  $K_t$  is the Temkin isotherm constant (L/g). These constants were obtained from plotting  $Q_e$  versus  $\ln(C_e)$  (figure 19 and 20). Values of  $Bt$  and  $K_t$  are listed in Table 2.

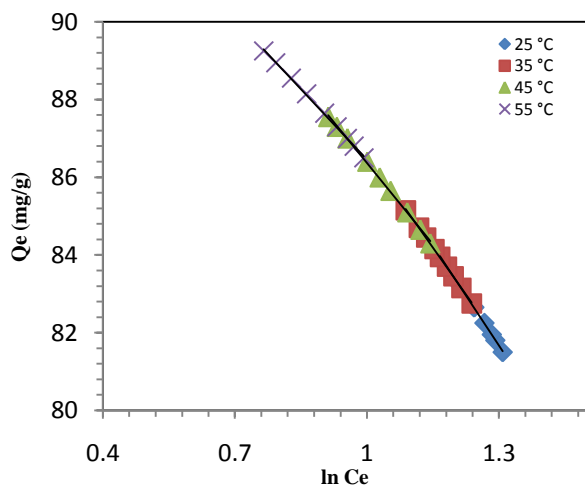


Figure 19: Temkin isotherm for RB adsorption onto RC

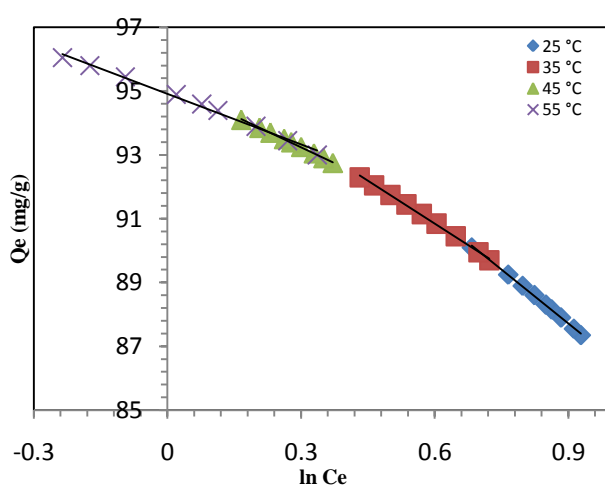


Figure 20: Temkin isotherm for RB adsorption onto MC

**Table 2:** Adsorption isotherm constants for RB adsorption onto RC and MC

T(C°)	Langmuir isotherm constants				Freundlich isotherm			Temkin isotherm			
	qm (mg/g)	K <sub>L</sub> (L.g <sup>-1</sup> )	R <sup>2</sup>	R <sub>L</sub>	K <sub>F</sub> (mg/g (L/mg) <sup>1/n</sup> )	n	R <sup>2</sup>	K <sub>t</sub> (L.g <sup>-1</sup> )	B <sub>t</sub> (KJ/mol)	R <sup>2</sup>	
RC	25	68.4932	-1.6782	0.9999	0.96648	107.103	-4.796	0.9996	0.00239	-17.249	0.9997
	35	70.4225	-1.9455	0.9999	0.96109	104.858	-5.238	0.9992	0.00165	-16.024	0.9995
	45	74.0740	-2.5472	0.9999	0.94906	101.624	-6.146	0.9986	0.00076	-13.989	0.999
	55	76.9230	-3.4211	0.9999	0.93152	99.197	-7.283	0.999	0.00028	-12.071	0.9991
MC	25	78.7400	-3.9688	0.9999	0.9206	98.333	-7.880	0.9996	0.00016	-11.254	0.9997
	35	82.6446	-6.3690	0.9999	0.8726	96.360	-10.172	0.9992	2.14x10 <sup>-5</sup>	-8.9471	0.9995
	45	86.9565	-11.5000	0.9999	0.7700	95.236	-14.224	0.9986	5.04 x10 <sup>-5</sup>	-6.566	0.999
	55	89.2857	-18.6670	0.9999	0.6266	94.907	-17.857	0.999	1.63 x10 <sup>-5</sup>	-5.2935	0.9991

3.6. Adsorption kinetics

Three simplified kinetic models were adopted to examine the mechanism of the adsorption process. First, the kinetics of adsorption was analyzed by the pseudo-first-order equation given by Lagergren [14] as:

$$\log(qe - qt) = \log(qe) - \left(\frac{k_1}{2.303}\right) t \quad (7)$$

Where  $q_e$  and  $q_t$  are the amounts of RB adsorbed (mg/g) at equilibrium and at time  $t$  (h), respectively, and  $k_1$  (g.mg<sup>-1</sup>.h<sup>-1</sup>) is the rate constant adsorption. Values of  $k_1$  at 25°C were calculated from the plots of  $\ln(q_e - q_t)$  versus  $t$  (figure 21 and 22) for different initial concentrations of RB. The  $R^2$  values obtained were relatively small and the experimental  $q_e$  values did not agree with the calculated values obtained from the linear plots (Table 3).

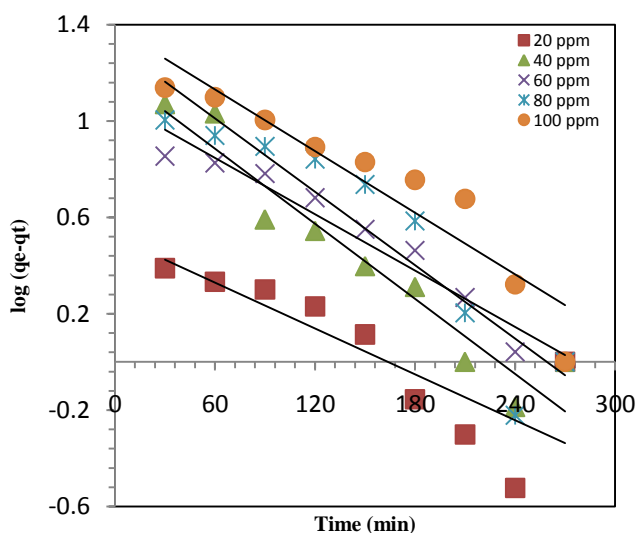


**Figure 21:** Pseudo-first order kinetic model for RB adsorption onto RC at different initial concentrations.

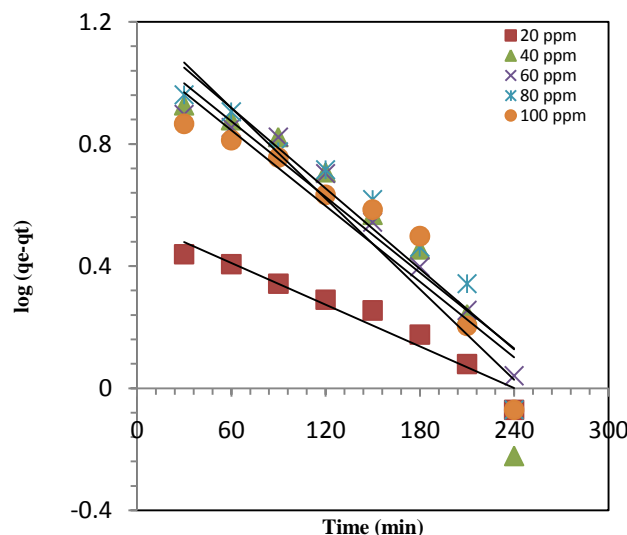


**Figure 22:** Pseudo-first order kinetic model for RB adsorption onto MC at different initial concentrations.

The pseudo-second-order equation based on equilibrium adsorption [15] is expressed as:

$$\frac{1}{qt} = \frac{1}{K_2 qe^2} + \left(\frac{1}{qe}\right) t \quad (8)$$

Where  $k_2$  ( $\text{g}\cdot\text{mg}^{-1}\cdot\text{h}^{-1}$ ) is the rate constant of second-order adsorption. The linear plot of  $t/q_t$  versus  $t$  at  $25^\circ\text{C}$ , as shown in (Figure 23 and 24), yielded  $R^2$  values that were vary of 0.9997 to 1 by RC and vary of 0.9998 to 1 for all RB concentrations adsorbed by MC. It also showed a good agreement between the experimental and the calculated  $q_e$  values (Table 3), indicating the applicability of this model to describe the adsorption process of RB onto RC and MC.

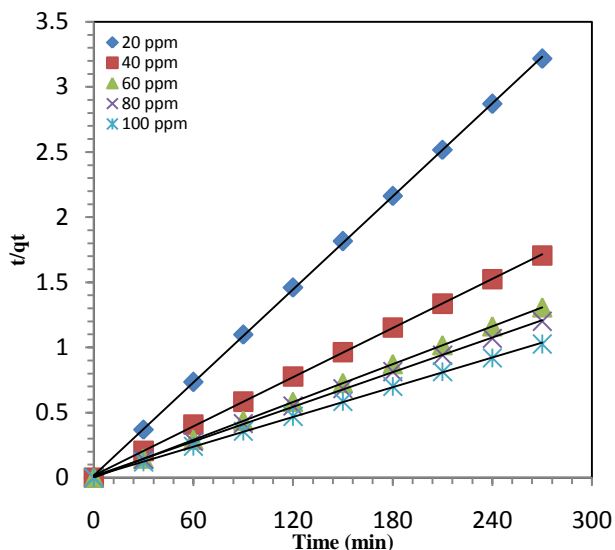


**Figure 23:** Pseudo-second order kinetic model for RB adsorption onto RC at different initial concentrations

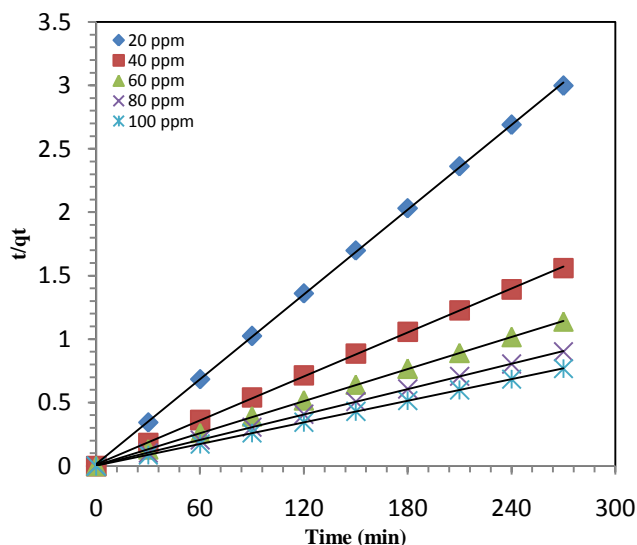


**Figure 24:** Pseudo-second order kinetic model for RB adsorption onto MC at different initial concentrations

Intra-particle diffusion model based on the theory proposed by Weber and Morris [16] was tested to identify the diffusion mechanism. According to this theory:

$$q_t = K_p t^{1/2} + C \quad (9)$$

Where  $C$  is the intercept and  $K_p$  is the intra-particle diffusion rate constant ( $\text{mol}\cdot\text{min}^{-1/2}\cdot\text{g}^{-1}$ ), is obtained from the slope of the straight line of  $q_t$  versus  $t^{1/2}$ .

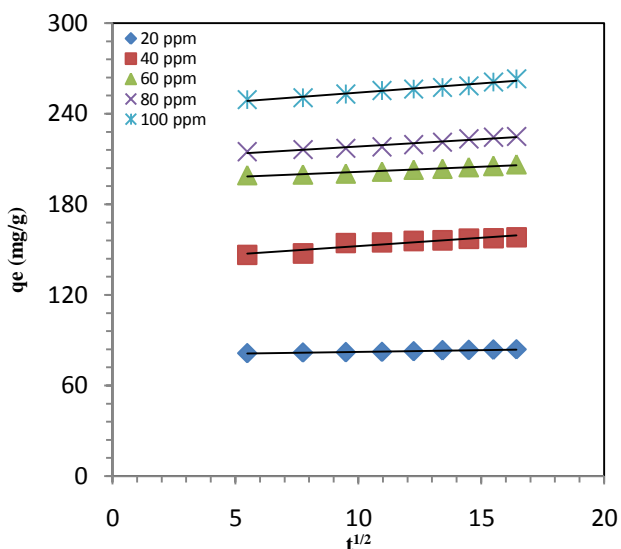


**Figure 25:** Intra-particle diffusion kinetic model for RB adsorption onto RC at different initial concentrations.

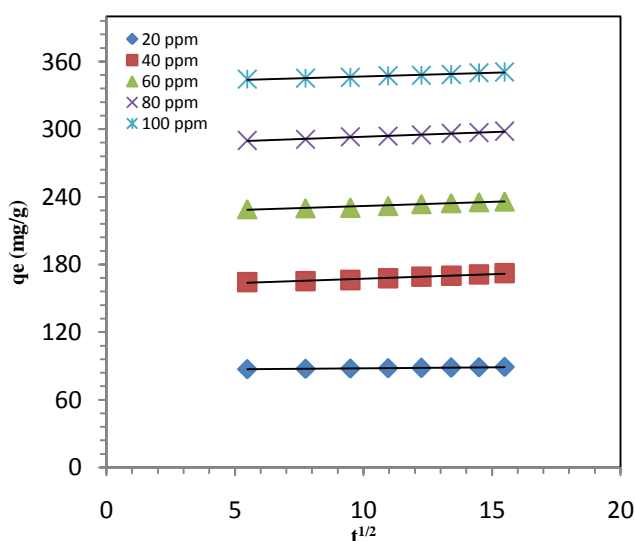


**Figure 26:** Intra-particle diffusion kinetic model for RB adsorption onto MC at different initial concentrations

**Table 3:** Pseudo-first-order, Pseudo-second-order and Intra-particle diffusion values.

Clay	C <sub>0</sub> (mg/L)	q <sub>e</sub> <sup>exp</sup> (mg/g)	Pseudo-first-order			Pseudo-second-order			Intra-particle diffusion		
			q <sub>e</sub>	K <sub>1</sub>	R <sup>2</sup>	q <sub>e</sub>	K <sup>2</sup>	R <sup>2</sup>	C	K <sub>i</sub>	R <sup>2</sup>
RC	20	83.95	4.3621	0.0101	0.6884	84.0336	0.0055	0.9999	79.9280	0.2374	0.9556
	40	158.25	18.6337	0.0136	0.9254	161.2903	0.0016	0.9998	141.3000	1.1013	0.8769
	60	206.45	11.7760	0.0088	0.9522	208.3333	0.0000	1.0000	194.6500	0.6820	0.9605
	80	225.00	21.6421	0.0122	0.8614	227.2727	0.0014	0.9997	208.4500	0.9823	0.9519
	100	263.15	20.0447	0.0078	0.8808	263.1579	0.0014	0.9997	241.7000	1.2248	0.9699
MC	20	90.10	3.5261	0.0076	0.9469	90.0900	0.0052	0.9998	85.220	0.2241	0.8974
	40	173.00	16.4021	0.0113	0.8815	175.4386	0.0016	0.9998	159.2400	0.8242	0.9795
	60	237.20	13.2709	0.0094	0.9532	238.0952	0.0017	0.9999	224.2600	0.7646	0.9678
	80	299.25	15.2090	0.0101	0.9100	303.0303	0.0019	0.9999	285.0300	0.8466	0.9901
	100	351.75	12.4194	0.0094	0.8912	357.1429	0.0022	1.0000	340.0000	0.6849	0.9694

### 3.7. Thermodynamic Studies

Thermodynamic parameters including Gibbs free energy change ( $\Delta G^\circ$ ), enthalpy change ( $\Delta H^\circ$ ), and entropy change ( $\Delta S^\circ$ ) was calculated from the following:

$$\Delta G^\circ = -RT \ln K_d(10)$$

$$\ln K_d = \frac{\Delta S^\circ}{R} - \frac{\Delta H^\circ}{RT}(11)$$

Where R is the ideal gas constant (8.314 J.mol<sup>-1</sup>.K<sup>-1</sup>), T is the absolute temperature (Kelvin), and K<sub>d</sub> is the distribution coefficient for adsorption.

Equation (10) is known as the Van't Hoff equation, and it expresses a relationship between equilibrium constant and temperature. Plots of lnK<sub>d</sub> versus 1/T (K<sup>-1</sup>) should be a straight line as shown in (figure 27 and 28).

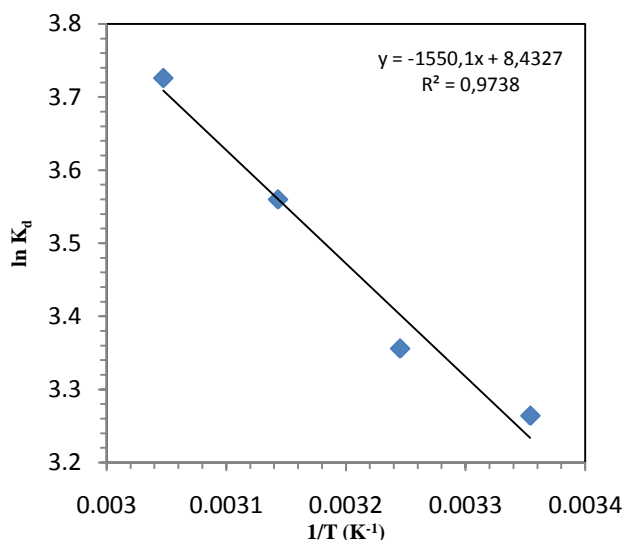


**Figure 27:** Plot of ln K<sub>d</sub> versus 1/T for the enthalpy change of the adsorption process for RC

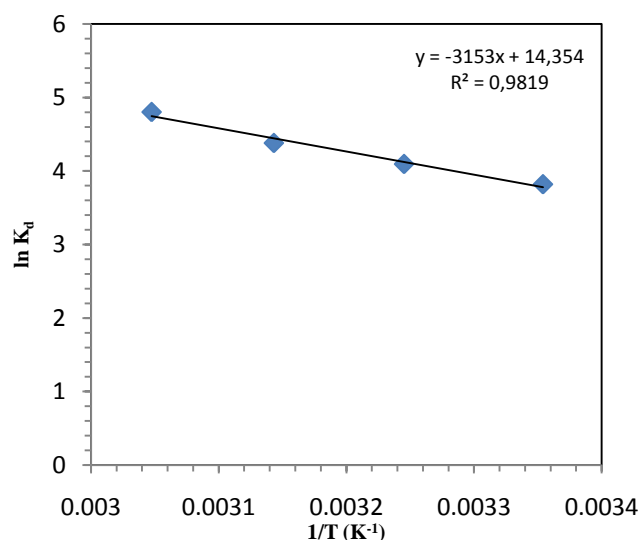


**Figure 28:** Plot of ln K<sub>d</sub> versus 1/T for the enthalpy change of the adsorption process for MC

The values of  $\Delta H^\circ$  and  $\Delta S^\circ$  for both RC and MC were calculated from the slope and intercept of Van't Hoff plot, respectively. The thermodynamic parameters associated with the adsorption of RB onto RC and MC are listed in Table 4.

The positive values of  $\Delta G^\circ$  suggest that adsorption reaction requires energy to carry out [17].

The positive value of  $\Delta H^\circ$  indicates the endothermic nature of the process. The  $\Delta S^\circ$  values were found to be positive which suggests an increase in the randomness at the solid/solution interface during the adsorption [18]. This further confirmed the endothermic nature of the process.

**Table 4:** Values of thermodynamics parameters for RB adsorption onto RC and MC

Clay	Temperature (K)	$\Delta G$ (KJ.mol <sup>-1</sup> )	$\Delta H$ (KJ.mol <sup>-1</sup> )	$\Delta S$ (KJ.mol <sup>-1</sup> .K <sup>-1</sup> )	R <sup>2</sup>
RC	298.15	8.016	12.887	0.0701	0.9738
	308.15	8.717			
	318.15	9.418			
	328.15	10.119			
MC	298.15	9.355	26.214	0.1193	0.9819
	308.15	10.548			
	318.15	11.741			
	328.15	12.934			

## Conclusions

The present study evaluates that raw and modified Moroccan natural clays can be used as a promising, effective adsorbent for the removal of RB from wastewater. The adsorption of RB was found to be dependent on the time of contact, solution temperature, initial concentration and pH of solution. The maximum removal of RB was found to be 83.95% when we used RC adsorbent and 90.10% with MC adsorbent.

The equilibrium adsorption data were best represented by the Langmuir isotherm, indication monolayer adsorption on a homogenous surface and values of  $q_{max}$  where increased from 68.49 to 76.92 mg/g for RC and 78.74 to 89.28 for MC. The adsorption kinetic was well described by the pseudo-second-order model.

The removal process of RB onto RC and MC is more spontaneous at upper temperatures, tends to be endothermic. Finally, the use of Moroccan natural clays shows a greater potential for the removal of textile dyes, as no costly equipment is required.

## References

- Banerjee S., Sharma G. C., Dubey S., Sharma Y. C., *J Mater Environ Sci*, 6 (2015), 2045–2052.
- El Haddad M., Regti A., Laamari M. R., Mamouni R., Saffaj N., *J Mater Environ Sci*, 5 (2014), 667–74.
- Pornaroonthama, Phuwadej, Nutthavich Thouchprasitchai, and Sangobtip Pongstabodee, *Journal of Environmental Management*, 157 (2015), 194–204.
- Tahiri, A., P. Montero, H. El Hadi, D. Martínez Poyatos, A. Azor, F. Bea, and others, *Journal of African Earth Sciences*, 57 (2010), 1–13.
- Vasquez, Erick S., Janice L. Cunningham, Justin B. McMahan, C. LaShan Simpson, and Keisha B. Walters, *J. Mater. Chem. B*, 3 (2015), 6411–19.
- Li, Qian, Rajini P. Antony, Lydia Helena Wong, and Dickon H. L. Ng, *RSC Adv.*, 5 (2015), 100142–46.
- Doğan M., Alkan M., Onganer Y., *Water, Air, and Soil Pollution*, 120 (2000), 229–248.
- Mahammed F., Benguella B., *J. Mater. Environ. Sci*, 7 (2016), 285–292.
- Ad C., Benalia M., Laidani Y., Elmsellem H., Henini G., Nouacer I., Djedid M., *J Mater Environ Sci*, 7 (2016) 319–330.
- Langmuir I., *J. Chem. Soc.*, 38 (1916) 2221–2295.
- Abd El-Latif M. M., Elkady M. F., *Desalination*, 255 (2010), 21–43.
- Freundlich H.M.F., *Physik. Chemie (Leipzig)*, 57A (1906) 385–470.
- Aharoni C., Ungarish M., *Journal of the Chemical Society, Faraday Transactions 1: Physical Chemistry in Condensed Phases*, 73 (1977), 456–464.
- Lagergren S., *Kungliga Svenska Vetenskapsakademiens Handlingar*, 24 (1898) 1–39.
- Ho Y. S., McKay G., *Chemical Engineering Journal*, 70 (1998), 115–24.
- MORRIS J. C., WEBER W. J., in *Advances in Water Pollution Research*, Pergamon, (1964), pp. 231–66.
- Ali R. M., Hamad H. A., Hussein M. M., Malash G. F., *Ecological Engineering*, 91 (2016), 317–32.
- Elmoubarki, R., F.Z. Mahjoubi, H. Tounsadi, J. Moustadraf, M. Abdennouri, A. Zouhri, and others, *Water Resources and Industry*, 9 (2015), 16–29.

(2017) ; <http://www.jmaterenvirosci.com>